PLANE STRESS DUCTILE FRACTURE

B. Cotterell and Y.W. Mai

Department of Mechanical Engineering,
University of Sydney,
Sydney. N.S.W. 2006
Australia.

ABSTRACT

The ductile fracture of thin metal sheets is illustrated with experiments on deeply notched specimens using two materials: one with a low strain hardening exponent and the other with a reasonably high one. It is shown that the J_R resistance curve can be estimated from simple tensile tests and that the initiation and the maximum value can be found by extrapolation of the specific work of initiation and propagation to zero ligament length. Materials that have a high strain hardening exponent show practically no increase in fracture resistance J_R with crack growth. Even in materials with low strain hardening exponents the increase in J_R with crack growth is slight.

KEYWORDS

Ductile fracture; J-integral; strain hardening; fracture work.

INTRODUCTION

Begley and Landes (1972) and Broberg (1971) have proposed that the J-integral (Rice, 1968) can be used as a ductile fracture criterion. Since the strain field ahead of the tip of a ductile crack in a strain hardening material is a unique function of J and the strain hardening exponent n (Rice and Rosengren, 1968; Hutchinson, 1968) the critical value of the J-integral is independent of the specimen geometry. Thus the J concept of post yield fracture mechanics (PYFM) parallels the K concept of linear elastic fracture mechanics (LEFM).

The strain field at the tip of a crack in a non strain hardening material is not unique, because strain localization can occur. Intense strain gradients can develop in low strain hardening materials and ductile fracture in such materials may not be accurately predicted by a one parameter criterion. There is a similar breakdown in LEFM for materials of low yield strength and high toughness, where a large plastic zone forms at the tip of the crack.

In thin ductile sheets, strain localization causes necks to form, which are analogous to the plastic zones in LEFM. It is assumed that, provided the J-integral is evaluated outside the necked zone, that PYFM applies and ductile tearing occurs when J reaches a critical value. The J-integral calculated for a contour within the process zone is dependent on the path as shown by McMeeking (1977). In this paper we further develop our concept of essential work (Cotterell and Reddel, 1977; Cotterell, 1977) and show its relationship to the J-integral and the crack tip displacement (CTOD) concept. Fracture experiments using two sheet materials, one a low alloy steel (Lyten) that has a small necked zone, and the other, a half hard commercial aluminium that has a large necked zone, are described. Most of the tests reported use deep double edge notched tension (DENT) specimens, but some results using a deeply cracked centre notch tension (DCNT) specimen are presented (see Fig. 1).

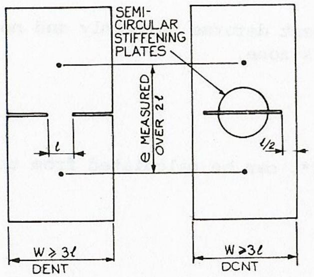

Fig. 1. Specimen geometry.

LOCALIZED NECKING IN THIN SHEETS

Ductile tearing in thin sheets is preceded by localized necking. When a thin sheet, with no stress raiser, is deformed the description of localized necking given by Hill (1952) predicts that necking occurs along a line of zero extension that is generally at an angle to the principal strain axes. The strain field ahead of the tip of a crack under mode I opening is a unique function of J and the strain hardening exponent n (Hutchinson, 1968) regardless of the overall geometry. The transverse strain tends to zero as the strain hardening exponent n diminishes (Hutchinson, 1968). Thus for low strain hardening materials, the initial neck development is in the direction of the crack, regardless of the overall geometry. In the DENT specimen the notch constrains the deformation so that the strain along the ligament is zero, and a neck can spread along the whole of the ligament. There is no such restraint in the DCNT specimen, and the necking for a plastic rigid material is along lines at an angle of approximately 35° to the crack line. However, for a strain hardening material, the initial neck formation is along the prolongation of the crack and only forks when the necked zone approaches the free edge.

It is assumed that a neck forms at the tip of a crack when the strain reaches a critical value ε_n which, for simplicity, is assumed to be equal to the strain at maximum load in a simple tension test, although the strain state is different. If d is the width of the pupative process zone that later forms the neck, then the crack tip opening displacement (CTOD), δ, at which necking starts is simply $\varepsilon_n d$. As the crack tip opening displacement increases, the necked zone grows from the crack tip and it is assumed that its length, ρ, up to the initiation of a ductile tear is given by

$$\rho = \frac{\delta - \varepsilon_n d}{\alpha} \qquad (1)$$

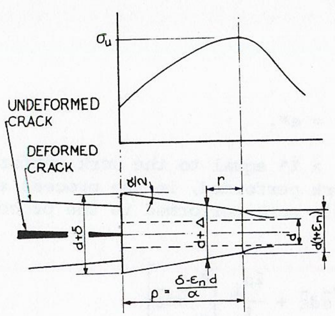

Fig.2. The necked process zone.

where α is a constant that depends mainly on the strain hardening exponent n and tends to zero as n tends to zero. Once the sheet necks, the load carried decreases and no further plastic straining occurs in the sheet outside this region. Thus the stretch Δ, in the necked zone is equal to the increase in CTOD (see Fig. 2)

and equation (1) implies that

$$\Delta - \varepsilon_n d = (\delta - \varepsilon_n d)\,\frac{r}{\rho} = \alpha r \qquad (2)$$

The width, d, of the pupative neck can be estimated from the thickness of the sheet t_f, after fracture. The reduction in thickness is uniform up to the point of necking when the thickness is given by

$$t = t_o(1 - \gamma\,\varepsilon_n) \qquad (3)$$

where t_o is the original sheet thickness and γ, for an isotropic material, lies between the limits $\frac{1}{2} < \gamma < 1$. In the DENT specimen Hill's theory (1952) predicts that there is no contraction between the notches and $\gamma = 1$. It is assumed that the neck can be modelled by a trapezoid and that during necking the transverse strain is zero. Thus the constancy of volume condition gives

$$d = \frac{\delta_R\,[t_o(1-\gamma\,\varepsilon_n) + t_R]}{[t_o(1+\gamma\,\varepsilon_n) - t_R]} \qquad (4)$$

which is of the order of the sheet thickness.

THE INITIATION OF A DUCTILE TEAR

It is assumed that the initiation of ductile tearing occurs when the CTOD reaches a critical value δ_i. If the specimen is sufficiently large, the length of the necked zone at initiation, ρ_i, is given by equation (1).

The Initiation Value of J

The value of the J-integral (Rice, 1968)

$$J = \oint_\Gamma \left[W\,dy - T_j\,\frac{\partial u_j}{\partial x}\,ds \right] \qquad (5)$$

at initiation, J_i, can be found by taking the integration around the edge of the necked zone. The strain energy density function, W, at the edge of this zone is constant, because the sheet is just on the point of necking and is given by

$$W = \int_0^{\bar\varepsilon_n} \bar\sigma\,d\bar\varepsilon \qquad (6)$$

where $\bar\sigma$ and $\bar\varepsilon$ are the true stress and strain. The traction, σ, on the necked zone is a function of the stretch, Δ. Thus

$$J_i = \int_0^d W\,dy + 2\int_0^\rho \sigma(\Delta)\,\frac{\alpha}{2}\,dr = d\int_0^{\bar\varepsilon_n} \bar\sigma\,d\bar\varepsilon + \int_{\varepsilon_n d}^{\delta} \sigma(\Delta)\,d\Delta \qquad (7)$$

which is equal to the work performed per unit area at the tip of the crack, previously called by us the specific essential work (Cotterell and Reddel, 1977 and Cotterell, 1977). Rice, Paris and Merkle (1973) suggest, on the basis of similarity, that the J-integral for fully yielded DENT and DCNT specimens can be estimated directly from a single load-elongation record and give the following expression (see Fig. 1).

$$J_i = \mathcal{G}_e + \frac{1}{\ell t}\left[2\int_o^{e_i} P\,de - P_i e_i\right] \tag{8}$$

where $\mathcal{G}_e$ is the elastic energy release rate, P is the load and e the plastic extension. However, in the ductile fracture of thin sheets there is no true geometric similarity, because of the necked process zone. If the necked zone is small compared with the ligament length, then we expect equation (8) to give a good approximation to J_i. The first term in the brackets of equation (8) is the specific plastic work of initiation w^i defined by

$$w^i = \frac{1}{\ell t}\int_o^{e_i} P\,de \tag{9}$$

This work, which is almost independent of the ligament length ℓ, can be partitioned into the specific work performed in the process zone w_e^i and the plastic work performed in the surrounding material w_p^i.

Strain in the Ligament

Since unloading takes place in the necked zone, only the material between necks undergoes plastic deformation upon further loading. Assuming that the plastic zone is roughly circular (Cotterell and Reddel, 1977) the strain increment at the centre (edge) of the ligament is approximately given by

$$d\varepsilon_o = \frac{de}{\ell - 2\rho} \tag{10}$$

Up to initiation, the CTOD is equal to the elongation e and equations (1) and (10) can be combined to give

$$\varepsilon_o = \varepsilon_n \frac{d}{\ell} - \frac{\alpha}{2}\ln\left[1 - \frac{2(e - \varepsilon_n d)}{\alpha \ell}\right] \tag{11}$$

If the ligament ℓ is large enough, the necked zone develops to ρ_i at initiation when $e = \delta_i$. However, for small ligaments ε_o reaches the critical necking strain ε_n before initiation, at which the necking suddenly spreads along the entire ligament. This sudden spread of necking is the result of our assumption that the length of the necked zone is always proportional to the CTOD. This proportionality strictly only holds if $\rho \ll \ell$. With small ligaments the necking accelerates as the necks approach one another (or the free edge), but the error caused by assuming proportionality for all ligament lengths is small. The critical ligament length ℓ* at which the entire ligament necks just before crack initiation is given by

$$\varepsilon_n\left(1 - \frac{d}{\ell^*}\right) = -\frac{\alpha}{2}\ln\left(1 - \frac{2\rho_i}{\ell^*}\right) \tag{12}$$

If the length of the ligament is less than ℓ*, the whole ligament necks when

$$e^* = \varepsilon_n d + \frac{\alpha \ell^*}{2}\left[1 - \exp - \frac{2}{\alpha}\varepsilon_n\left(1 - \frac{d}{\ell^*}\right)\right] \tag{13}$$

For elongations greater than e*, the whole ligament deforms uniformly and no further plastic strain occurs outside the process zone.

Specific Work of Initiation

The load P_n carried by the necked zone, if $\ell > \ell^*$, can be calculated from the stretch, Δ, in the process zone and is

$$P_n = t_o \int_o^{\rho} \sigma(\Delta)\,dr \tag{14}$$

where Δ is given by equation (2). The strain between the necked zones varies from ε_o at the centre (edge) to ε_n at the edge of the necked zone. A weighted average strain over the unnecked ligament

$$\varepsilon_{av} = C\varepsilon_o + (1 - C)\,\varepsilon_n, \tag{15}$$

where $C < 1$ is the weighting constant, enables the load on the unnecked ligament P_p to be calculated:

$$P_p = (\ell - 2\rho)\,t_o\,\bar{\sigma}(\bar{\varepsilon}_{av})(1 - \bar{\varepsilon}_{av}) \tag{16}$$

where the approximation $\exp(-\bar{\varepsilon}_{av}) = (1 - \bar{\varepsilon}_{av})$ has been made. Thus the total load $(P_n + P_p)$ can be calculated and the specific work of initiation w^i calculated by integration of the load-elongation expression. If $\ell < \ell^*$, $P_p = 0$ for $e > e^*$, P_n is given by:

$$P_n = t_o \int_o^{\ell} \sigma(\Delta)\,dr \tag{17}$$

and Δ is given by:

$$\Delta = \Delta^* + (e - e^*) \tag{18}$$

where Δ* is the stretch in the necked zone at e = e*.

The work performed in the process zone is for $\ell > \ell^*$ equal to the work performed in the necked zone up to initiation plus the work performed, in the process zone of width d, between the necks. Thus the specific work performed in the process zone is

$$w_e^i = \frac{2}{\ell}\int_o^{\rho_i}\int_o^{\Delta}\sigma(\Delta)\,d\Delta\,dr + d\left[\int^{\bar{\varepsilon}_{av}}\bar{\sigma}\,d\bar{\varepsilon} + \frac{2\rho_i}{\ell}\int_{\bar{\varepsilon}_{av}}^{\bar{\varepsilon}_n}\bar{\sigma}\,d\bar{\varepsilon}\right] \tag{19}$$

The expression for w_e^i when $\ell < \ell^*$ requires modification which give in the limit

$$w_e^i \longrightarrow J_i \qquad (20)$$

as $\ell \to 0$

The specific plastic work of initiation can be found from the difference

$$w_p^i = w^i - w_e^i \qquad (21)$$

THE PROPAGATION OF A DUCTILE TEAR

It is easiest to discuss propagation from the CTOD concept. The constraint caused by the notch enables initiation to occur with less reduction in thickness and generally at a smaller CTOD than propagation. Thus it is assumed that the initiation CTOD, δ_i, increases to δ_p during propagation through the distance, s, which is taken for the reduction in sheet thickness to reach its maximum. Typically s is equal to two sheet thicknesses. It is assumed, for simplicity, that the CTOD increases from δ_i to δ_p linearly and hence the CTOD is given by

$$\delta_R = \delta_i + (\delta_p - \delta_i)\frac{a}{s}$$

for a crack growth $a < s$ and

$$\delta_R = \delta_p \qquad (22)$$

for $a > s$.

It is assumed that the length ρ of the necked zone continues to be given by equation (1).

<u>Total Elongation to Fracture for DENT Specimens</u>

Consider first ligament lengths larger than ℓ^*, but small enough to be fully yielded before crack initiation. Assuming that the necked zone is as shown in Fig. 2, it is necessary to stretch the specimen by a further

$$\Delta e = e - \delta_i = (\delta_R - \delta_i) + \alpha a \qquad (23)$$

in order to extend the crack by a, if the CTOD increases to δ_R. The strain increment $d\varepsilon_o$ at the centre of the ligament is again given by equation (10) and integration yields

$$\varepsilon_o = \varepsilon_n \frac{d}{\ell} - \frac{\alpha}{2} \ln\left(1 - \frac{2\rho_R}{\ell} - \frac{2a}{\ell}\right) \qquad (24)$$

where the length of the necked zone ρ_R is given by

$$\rho_R = \frac{\delta_R - \varepsilon_n d}{\alpha} \ . \qquad (25)$$

Propagation continues until ε_o reaches the critical necking strain ε_n and the crack growth is a^*, the fracture is then completed by a further elongation of $(\delta_p - \varepsilon_n d)$. Hence the total elongation to fracture is given by

$$e_f = \delta_R + \delta_p - \varepsilon_n d + \alpha a^* , \qquad (26)$$

where δ_R is a function of a^*. If $\ell < \ell^*$ the whole ligament necks before crack initiation at an elongation e^* (equation (12)). A further elongation of $(\delta_R - \varepsilon_n d)$, where δ_R is now a function of $\ell/2s$, completely fractures the specimen. Thus the total elongation to fracture is given by

$$e_f = \delta_R + \frac{\ell\alpha}{2}\left\{1 - \exp - \frac{2}{\alpha}\varepsilon_n\left(1 - \frac{d}{e}\right)\right\} \qquad (27)$$

<u>The J_R Resistance Curve</u>

The J_R resistance curve can be calculated by again taking the contour of the J integral around the necked zone. Thus we obtain

$$J_R = d\int_0^{\varepsilon_n} \bar{\sigma} d\bar{\varepsilon} + \int_{\varepsilon_n d}^{\delta_R} \sigma(\Delta)\, d\Delta \qquad (28)$$

which is equal to the work performed per unit area at the tip of the crack and becomes a maximum when $a = s$.

<u>The Specific Work of Fracture</u>

The total load on the specimen can be calculated in exactly the same way as indicated in the section on initiation and the load-elongation expression integrated to give the specific work of fracture propagation w^p. Thus the total specific work of fracture is given by

$$w^f = w^i + w^p = w_e^i + w_p^i + w_e^p + w_p^p \qquad (29)$$

We will show that the relationship of w^f to the ligament length has the same form as previously suggested namely

$$w^f = J_p + \frac{\alpha}{2}\ell \qquad (30)$$

for $\ell > 2s$. The specific work of propagation performed in the surrounding plastic zone w_p^p also tends to J_p as ℓ tends to infinity.

THE DUCTILE FRACTURE OF TWO SHEET MATERIALS

Two sheet metals: a low alloy steel, Lyten, with a reasonably large strain hardening exponent and a small necked zone and a half hard commercial aluminium, AA2S, with a small strain hardening exponent and a large necked zone, both nominally 1.6 mm thick, have been chosen to illustrate plane stress ductile fracture. Tests were made with rolling direction normal to the applied tension for the Lyten sheet and parallel for the AA2S sheet. The mechanical properties of the two materials are summarized in Table 1.

The main geometry used was the DENT with ligaments small enough to ensure complete plastic flow before initiation and notches deep enough to limit yielding to the ligament as previously described (Cotterell and Reddel, 1977). Some initiation tests were made using DCNT geometry with semi circular stiffening plate attached to the notch edges to prevent buckling (see Fig. 2). The test results are summarized in Table 2.

TABLE 1 Mechanical Properties

		Lyten	AA2S
Yield strength	MPa	365	102
Ultimate strength	MPa	524	139
Strain at U.T.S.	%	17.5	3.6
Elongation on 50 mm	%	32.3	7.5

TABLE 2 DENT Results

	Lyten	AA2S
Reduction in thickness at initiation %	12	24
Reduction in thickness for propagation %	36	76
Process zone width d in mm	1.32	1.74
α	0.093	0.022
$\alpha^1 = \alpha + \dfrac{\delta_p - \delta_i}{s}$	0.093	0.162
ρ_i in mm	4	34
ρ_p in mm	4	49
C	0.9	0.67
$\dfrac{d}{\sigma_u \delta_i} \int_0^{\varepsilon_n} \sigma \, d\varepsilon$	0.404	0.079
$J_i/\sigma_u \delta_i$	0.833	0.859
$J_p/\sigma_u \delta_i$	0.833	0.985

Elongation to Initiation and Fracture

The plastic elongation for initiation and fracture are shown in Fig. 3 and Fig. 4. The elongation to initiation is independent of the ligament length apart from the scatter caused by inaccuracies in the visual detection of initiation and except for very small ligaments, where there is a partial transition to plane strain, is in keeping with the CTOD concept.

The elongation to fracture is a linear function of the ligament length, except for very small ligaments, for both Lyten and AA2S. However, whereas the intercept at zero ligament length for Lyten is the initiation CTOD δ_i, the intercept for AA2S is greater than δ_i. It is assumed that the zero intercept of the elongation to fracture is the CTOD of a fully developed propagating fracture, δ_p. It is

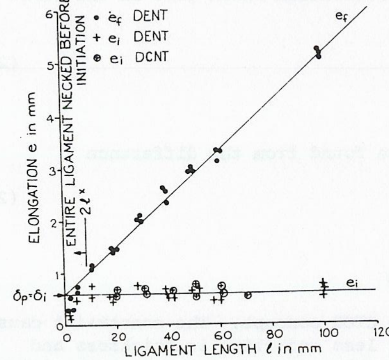

Fig. 3. The elongation of deeply notched Lyten sheets.

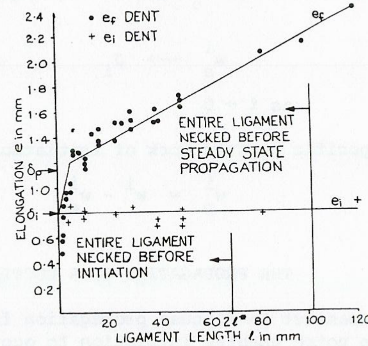

Fig. 4. The elongation of deeply notched AA2S sheets.

believed that the initiation and propagation values of the CTOD are practically identical for Lyten, because the reduction in thickness is small (see Table 2), and therefore, there is little thickness constraint. The thicknesses of the process zone, d, have been calculated using δ_p and t_R from equation (4) and are shown in Table 2.

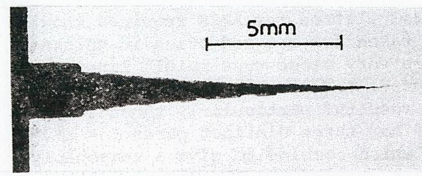

Fig. 5. Section of partial fracture in Lyten.

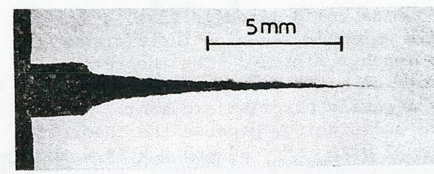

Fig. 6. Section of partial fracture in AA2S.

The slope of the straight line relationship between the elongation to fracture and the ligament length is assumed to be $\alpha/2$. A direct measure of α can be obtained from the angular opening of the crack. Mid thickness sections of partially fractured DENT specimens are shown in Figs. 5 and 6. The Lyten fracture shows a constant angular opening of $\tan^{-1}0.133$ which is greater than that estimated from the elongation to fracture (α = 0.093). The AA2S specimen shows a bell-mouthed crack opening, which is in keeping with a CTOD for propagation greater than that for initiation. The angular opening over the first 4 mm is $\tan^{-1}0.210$ which should be compared with $\alpha^1 = \alpha + (\delta_p - \delta_i)/s = 0.162$, whereas the angular opening at deeper crack depths is $\tan^{-1}0.055$ which should be compared with $\alpha = 0.022$. Thus the value of α obtained from direct measurement is greater than that obtained from the elongation to total fracture, which suggests that de/da is not strictly constant, but that the rate of crack growth increases towards the final stages of crack propagation. In subsequent calculations the values of α obtained from the elongation to fracture data are used, because these give the average rate of crack growth.

An estimate of the length of the necked zone can be obtained from equation (1). It is difficult to estimate the length of the necked zone precisely by direct measurement, because the end of the zone is ill defined. However, the thinning at the tip of a crack is shown in Figs. 7 and 8. It would appear (compare Table 2) that the present theory underestimates the critical length of the necked zone for Lyten and overestimates it for AA2S. Subsequent calculations are based on the lengths estimated from α.

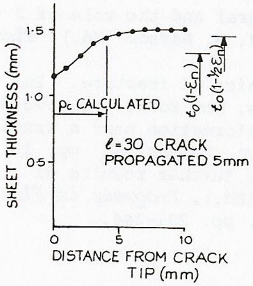

Fig. 7. Sheet thickness at the tip of a crack in Lyten.

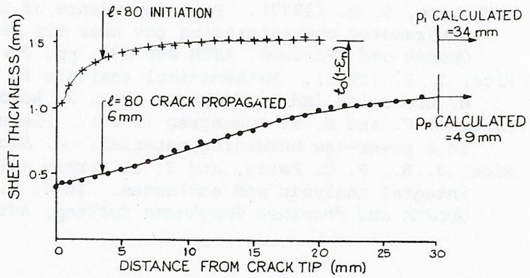

Fig. 8. Sheet thickness at the tip of a crack in AA2S.

The elongation to fracture has been calculated from equations (26) and (27) and is shown as solid lines in Figs. 3 and 4. The calculation for AA2S requires knowledge of s which is taken as the distance (2.5 mm) taken for the reduction in thickness to reach a minimum. The theoretical lines are very close to straight lines with a slope of $\alpha/2$ and a zero intercept δ_p. Of course, the results have been obtained by a partly circular argument. However, the results, particularly those for AA2S, are encouraging, because the theoretical line has three distinct parts $\ell < \ell^*$, $\ell > \ell^*$ with $a^* < s$, and $\ell > \ell^*$ with $a^* > s$ which combine to give a reasonably straight line. For ligaments less than about 10 mm the experimental results deviate from the theoretical lines, because of the partly plane strain nature of the fracture.

The J_R Resistance Curve

The value of J_R can be obtained from equation (28). The first integral in this equation can be found from a simple tension test. In order to avoid a discontinuity in the stress at the edge of the necked zone, the true stress-strain relationship is assumed to be

$$\frac{\bar{\sigma}}{\sigma_u} = \frac{1}{(1 - \varepsilon_n)} \left(\frac{\varepsilon}{\varepsilon_n}\right)^{\varepsilon_n} \qquad (31)$$

where the slight difference between true and engineering strain has been ignored and σ_u is the ultimate tensile strength. The width of the process zone is found from equation (4) using the values of δ_p and t_R listed in Table 2. Strain gauge measurements show that the transverse strain in the DENT specimen is small and thus $\gamma = 1$. The work performed during necking, which forms the second integral in equation (28) can be found from a shallow edge notch specimen with a ligament small enough to induce almost uniform necking. A fracture initiates in these specimens with a further stretch close to $(\delta_i - \varepsilon_n d)$. An empirical expression for the nominal stress in these specimen is

$$\sigma(\Delta) = \sigma_u \left[1 - \left(\frac{\Delta - \varepsilon_n d}{\delta_p - \varepsilon_n d}\right)^m\right] \qquad (32)$$

where $m \approx 2.4$ for Lyten and $m \approx 2.0$ for AA2S. The values of J_i and J_p are given in Table 2 and the J_R curve assuming that δ_R is given by equation (22) is presented in Fig. 9.

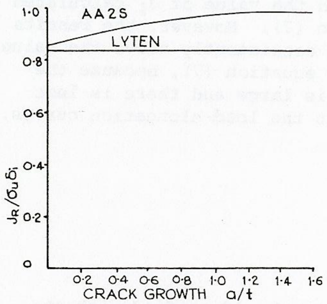

Fig. 9. The J_R resistance curve for Lyten and AA2S.

The Specific Work of Initiation and Fracture

The specific work of initiation and fracture, obtained by integration of the load-elongation, curves is shown in Figs. 10 and 11. The average value of the specific work of initiation for ligaments greater than about 10 mm is very close to J_i. The line of best fit to the specific work of fracture for ligaments greater than 10 mm has a zero intercept close to J_p.

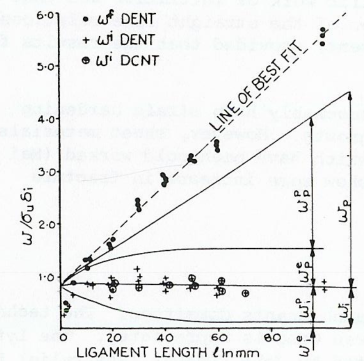

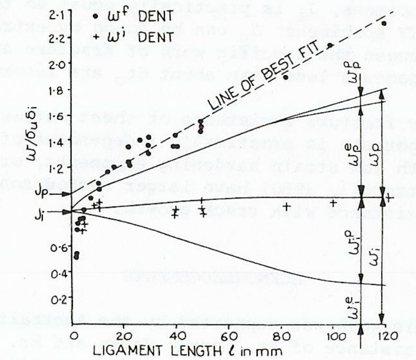

Fig. 10. Specific work of initiation and fracture for Lyten.

Fig. 11. Specific work of initiation and fracture for AA2S.

The theoretical components of the specific works of fracture are shown as full lines in Figs. 10 and 11. The value of the strain weighting constant C was chosen so that the theoretical maximum load gave the best fit to the experimental loads for ligament lengths greater than 10 mm. It is reasonable that C should be smaller for AA2S, because this sheet has the smaller strain hardening exponent and consequently the strain gradient in the unnecked ligament should be less. The specific work of initiation is accurately predicted, but the specific work of fracture is underestimated, because the load is underestimated during the early stages of propagation since we use an average value of α.

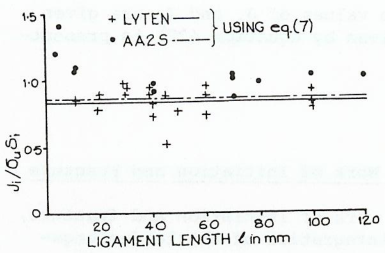

Fig. 12. J_i calculated from energy considerations.

The initiation of J integral J_i has been calculated from the specific work of initiation, w^1, using equation (8) and is shown in Fig. 12. The results for Lyten agree reasonably well, apart from the scatter, with the value of J_i calculated from equation (7). However, the results for AA2S lie consistently above the value predicted by equation (7), because the necked zone is large and there is less similarity in the load-elongation curves.

CONCLUSIONS

In plane stress ductile fracture, the process zone can be identified with the necked region at the tip of the crack. An expression for the J-integral can be obtained by taking the contour around the edge of the necked zone and evaluated from simple tensile tests. Provided that the necked zone is reasonably small, the J integral can also be calculated from a single load-elongation record obtained from a deeply notched specimen. It is also shown that, for DENT and DCNT specimens, J_i is practically equal to the specific work of initiation and that for DENT specimens, J_p can be found by extrapolation of the straight line relationship between the specific work of fracture and ligament, provided that the results for ligaments less than about $6t_o$ are ignored.

The fracture resistance of sheet metals with reasonably high strain hardening exponents is practically independent of crack growth. However, sheet materials with low strain hardening exponents, or those which have been cold worked (Mai and Cotterell, 1980) have larger necked zones and show some increase in fracture resistance with crack growth.

ACKNOWLEDGEMENTS

This work was supported by the Australian Research Grants Committee. The technical assistance of Mr. George Zajko and Mr. Thanh Tran Cong is appreciated. The Lyten sheet used in these tests were generously donated by John Lysaght (Australia) Ltd.

REFERENCES

Begley, J. A. and J. D. Landes (1972). The J integral as a fracture criterion. In H. T. Corten (Ed.), *Fracture Toughness*, American Society for Testing and Materials, ASTM STP 514, pp. 1-23.

Broberg, K. B. (1971). Crack growth criteria and non-linear fracture mechanics. *J. Mech. Phys. Solids*, 19, pp. 407-418.

Cotterell, B. and J. K. Reddel (1977). The essential work of plane stress ductile fracture. *Int. J. Frac.*, 13, pp. 267-277.

Cotterell, B. (1977). Plane stress ductile fracture. In G. C. Sih and C. L. Chow (Eds.), *Fracture Mechanics and Technology*, Vol. 2, Sijthoff and Noordhoff, Alphen aan den Rijn, pp. 785-795.

Hill, R. (1952). On discontinuous plastic states, with special reference to localized necking in thin sheets. *J. Mech. and Phys. Solids*, 1, pp. 19-30.

Hutchinson, J. W. (1968). Plastic stress and strain fields at a crack tip. *J. Mech. and Phys. Solids*, 16, pp. 337-347.

Mai, Y. W. and B. Cotterell (1980). Effects of prestrain on plane stress ductile fracture in α-brass. To be published in *J. Mat. Sci.*

McMeeking, R. M. (1977). Path dependence of the J integral and the role of J as a parameter characterising the near-tip field. In J. M. Barsom (Ed.), *Flaw Growth and Fracture*, ASTM STP 631, pp. 28-39.

Rice, J. R. (1968). Mathematical analysis in the mechanics of fracture. In H. Liebowitz (Ed.), *Fracture*, Vol. 2, Academic Press, New York. pp. 192-308.

Rice, J. R. and G. F. Rosengren (1968). Plane strain deformation near a crack tip in a power-law hardening material. *J. Mech. and Phys. Solids*, 16, pp. 1-12.

Rice, J. R., P. C. Paris, and J. G. Merkle (1973). Some further results of J integral analysis and estimates. In J. G. Kaufman (Ed.), *Progress in Flaw Growth and Fracture Toughness Testing*, ASTM STP 536, pp. 231-244.